

# Weak Mode Alignment in the CMS Tracker

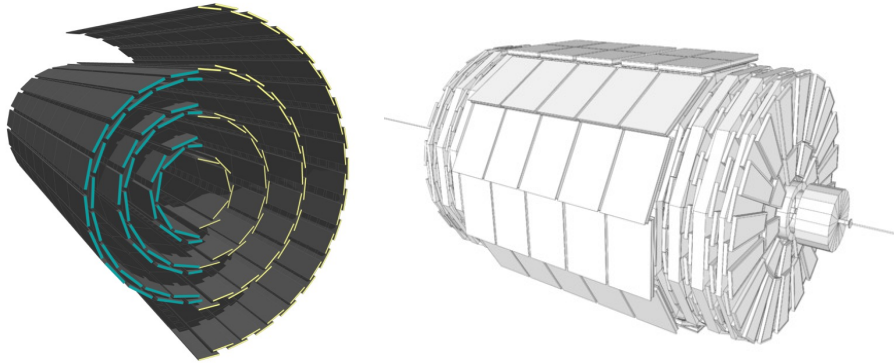
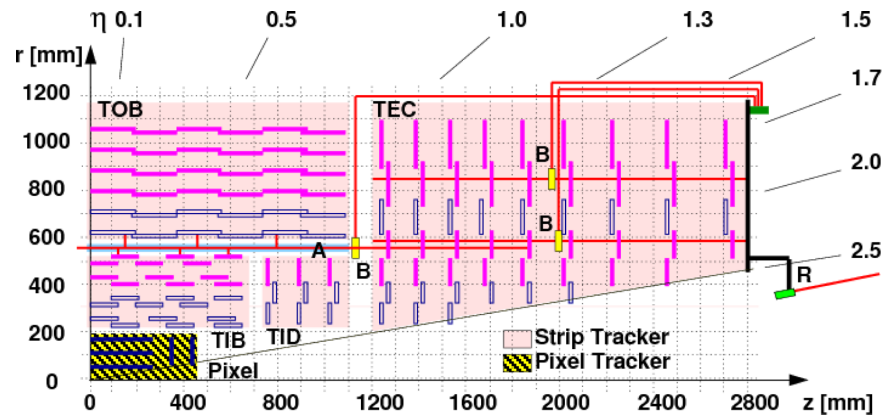
第三组：李一凡 刘白羽 刘怡芮

# Outline

---

- Background
- Weak Modes in CMS Detector
- Detection and Alignment Methods
- Verification and Performance
- Summary

# Background



- The CMS tracker is an all-silicon tracking detector located inside a 3.8 T solenoid. It contains 1440 pixel modules in 2016, and 1856 pixel modules after the Phase-1 pixel upgrade, together with 15148 strip modules, contribute  $\sim 200,000$  alignment parameters.
- The intrinsic hit resolution is at the level of  $O(10 - 30 \mu\text{m})$ , while the mechanical installation precision is only  $O(0.1 \text{ mm})$ .

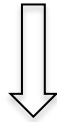
The alignment constants therefore have to describe module positions, orientations, and surface deformations with a precision significantly better than the hit resolution. In addition, Run 2 introduced stronger time dependence: pixel-detector interventions, magnet cycles, local calibration changes, and radiation damage can all mimic or induce coherent distortions.

# Background

Track based alignment - Construct  $\chi^2$  and minimize:

$$\chi^2(p, q) = \sum_{\text{tracks } j} \sum_{\text{hits } i} \left( \frac{\text{measure}_{ij} - \text{reconstruct}_{ij}(p, q_j)}{\sigma_{ij}^m} \right)^2$$

$p$  and  $q$  stand for alignment and track parameters separately.

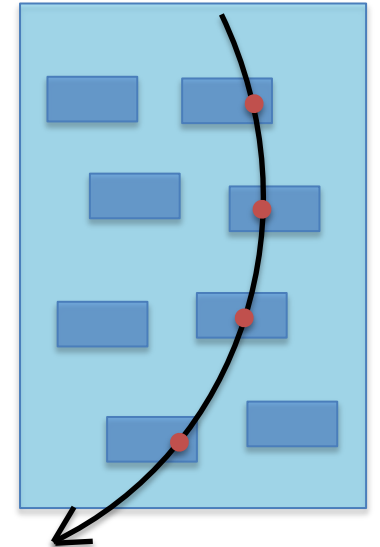
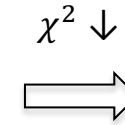
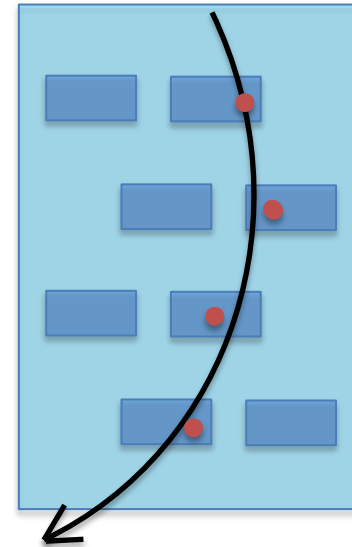


$$\begin{pmatrix} C_{pp} & C_{pq} \\ C_{qp} & C_{qq} \end{pmatrix} \begin{pmatrix} \Delta p \\ \Delta q \end{pmatrix} = \begin{pmatrix} b_p \\ b_q \end{pmatrix}$$

**Schur Complement**



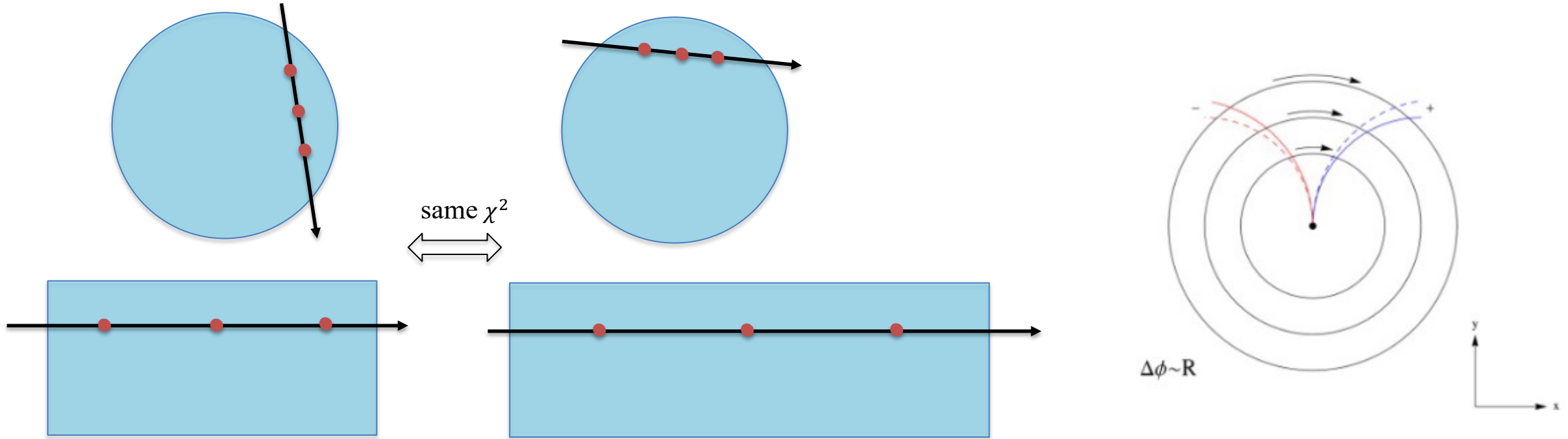
$$\begin{pmatrix} C' & 0 \\ * & * \end{pmatrix} \begin{pmatrix} \Delta p \\ * \end{pmatrix} = \begin{pmatrix} b' \\ * \end{pmatrix}, \quad C' = C_{pp} - C_{pq}C_{qq}^{-1}C_{qp} \quad \Longrightarrow \quad \text{Solve } p$$



This primarily fixes local and random displacement

# Background

However due to extra degree of freedom there are distortion modes satisfy  $\Delta\chi^2 \approx 0$  (Weak Modes) :



individual track  $\chi^2$  looks perfect, but **correlations between tracks are biased** → physics measurements distorted

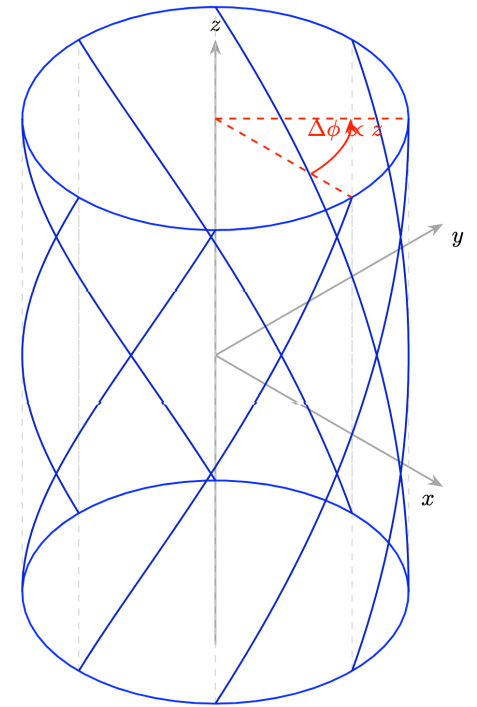
Alignment methods work for Weak Modes needed.

# Weak Modes in CMS Detector

CMS parameterizes first-order coherent distortions in cylindrical coordinates. The columns correspond to which coordinate is displaced:  $z$ ,  $r$ , or  $\phi$ . The rows correspond to which coordinate the displacement depends on:  $z$ ,  $r$ , or  $\phi$ .

Dependence	$\Delta z$	$\Delta r$	$\Delta \phi$
vs. $z$	z expansion: $\Delta z = \epsilon z$	bowing: $\Delta r = \epsilon r(z_0^2 - z^2)$	twist: $\Delta \phi = \epsilon z$
vs. $r$	telescope: $\Delta z = \epsilon r$	radial: $\Delta r = \epsilon r$	layer rotation: $\Delta \phi = \epsilon r$
vs. $\phi$	skew: $\Delta z = \epsilon \cos(\phi + \phi_0)$	elliptical: $\Delta r = \epsilon r \cos(2\phi + 2\phi_0)$	sagitta: $\Delta \phi = \epsilon \cos(\phi + \phi_0)$

Twist  
 $\Delta \phi = 25 \cdot z$



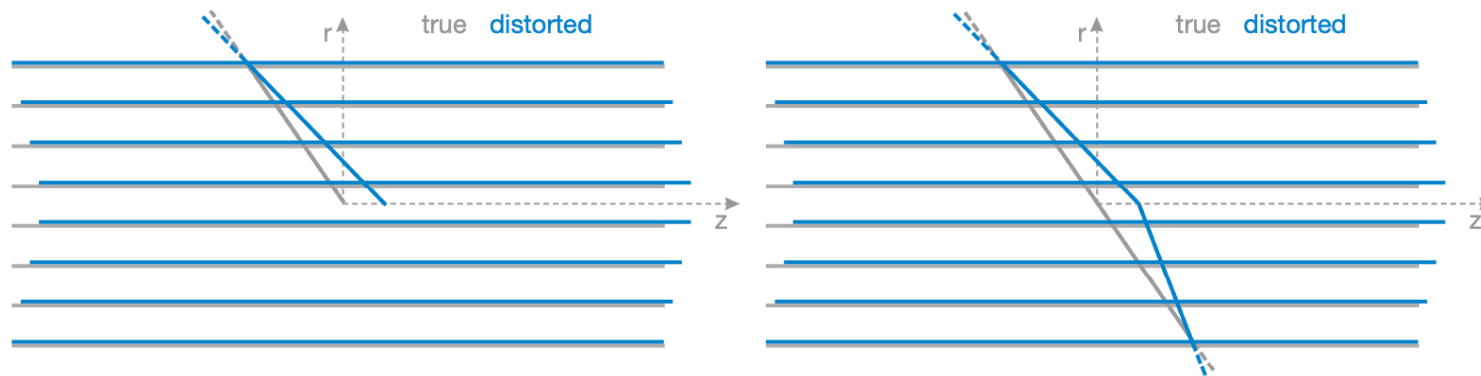
$\epsilon$  is a single parameter controlling each mode;  $z_0 \approx 272$  cm (half-length of the CMS tracker)

# Detection Method / Cosmic Ray

## Cosmic Ray (Muons):

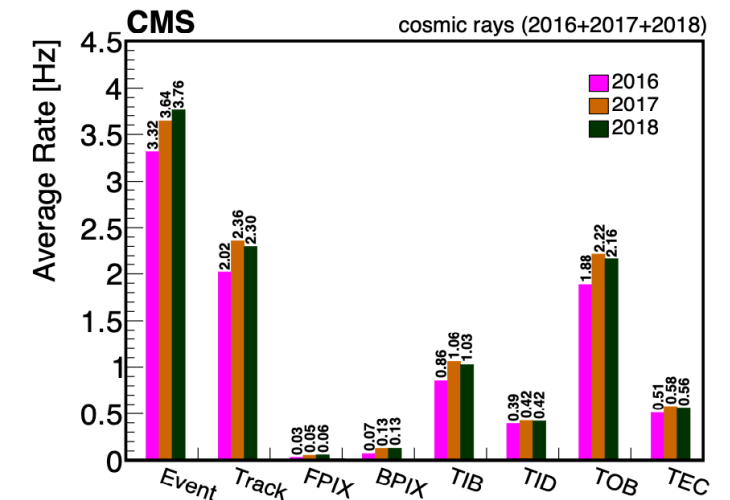
Muon track breaks cylindrical symmetry. Highly sensitive to **Telescope, Layer rotation, Skew, Elliptical, and Sagitta**

A cosmic ray muon traversing the top and bottom halves of the tracker. Split track at the point of closest approach, reconstruct them independently, then compare parameters from upper half vs. lower half



Difference in track parameters at the origin:  $\Delta\theta, \Delta d_z, \Delta d_{xy}, \Delta\left(\frac{q}{p_T}\right), \Delta\Phi$

In a perfectly aligned detector, these differences should average to zero.

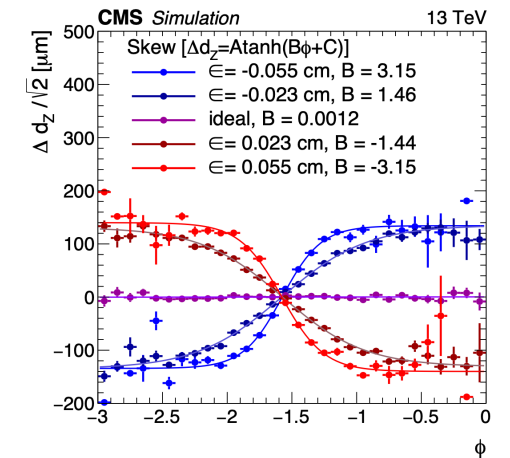
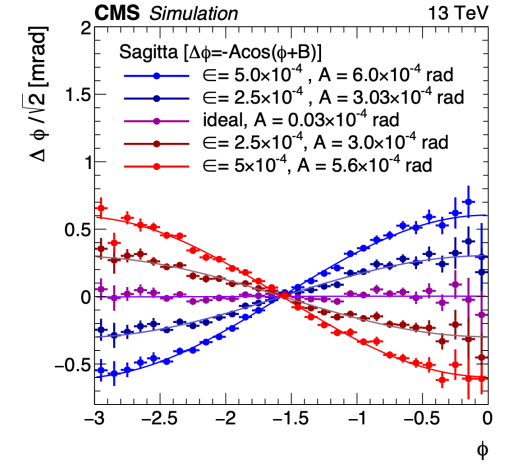
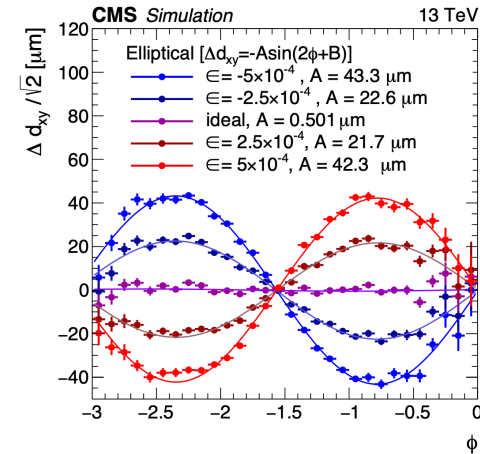
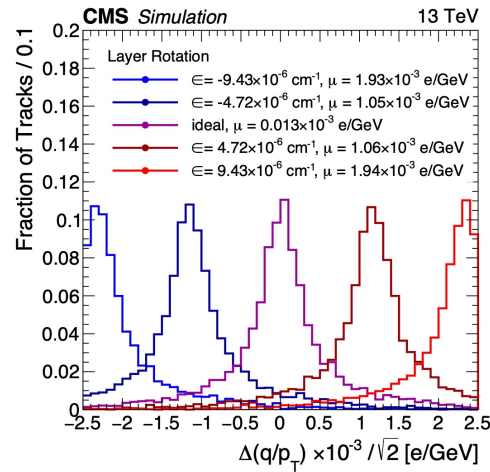
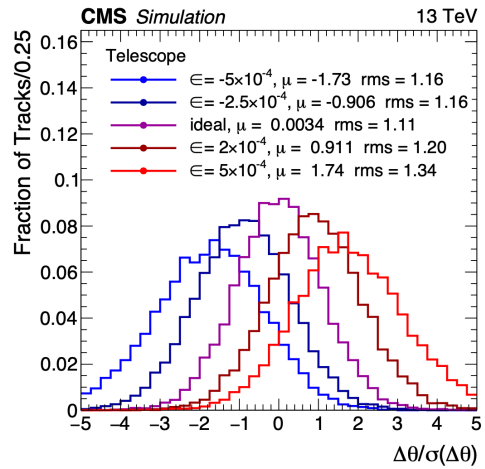


Rate of Cosmic Muon events in different area.

# Detection Method / Cosmic Ray

Powerful method valid in telescope, layer rotation, skew, elliptical and sagitta.

Blind to WMs that preserve track continuity (e.g., Uniform rotation or expansion)



**Mean Shifts:** Telescope and Layer Rotation cause global systematic shifts from zero.

**Modulations:** Skew, Elliptical, and Sagitta introduce distinct sinusoidal modulations as a function of the azimuthal angle

# Detection Method / Module Overlaps

## Module Overlaps:

Utilize tracks passing through overlapping modules within the same detector layer. Small distance between hits heavily reduces track parameter propagation uncertainties.

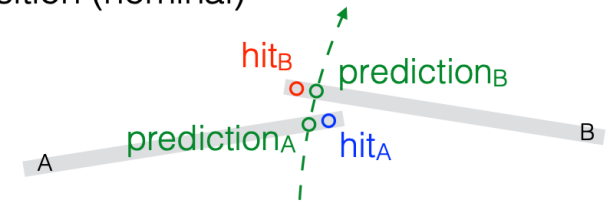
Double difference of residuals becomes independent of track parameters  $q$ :

$$\Delta r_A = \Delta(\text{hit}_A - \text{prediction}_A) = \frac{\partial f_A}{\partial p_A} \Delta p_A + \frac{\partial f_A}{\partial q_A} \Delta q, \quad \Delta r_B = \Delta(\text{hit}_B - \text{prediction}_B) = \frac{\partial f_B}{\partial p_B} \Delta p_B + \frac{\partial f_B}{\partial q_B} \Delta q,$$

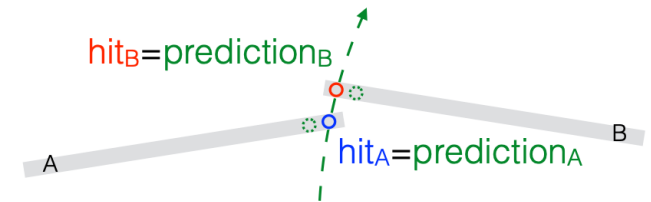
Track propagation error cancels out:  $\partial f_A / \partial q_A \approx \partial f_B / \partial q_B$

$$\Delta r_{AB} = \Delta r_A - \Delta r_B \approx \frac{\partial f_A}{\partial p_A} \Delta p_A - \frac{\partial f_B}{\partial p_B} \Delta p_B,$$

expected position (nominal)

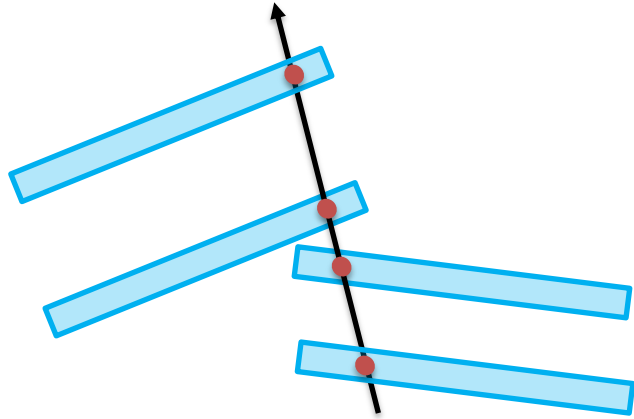


actual position (expansion)

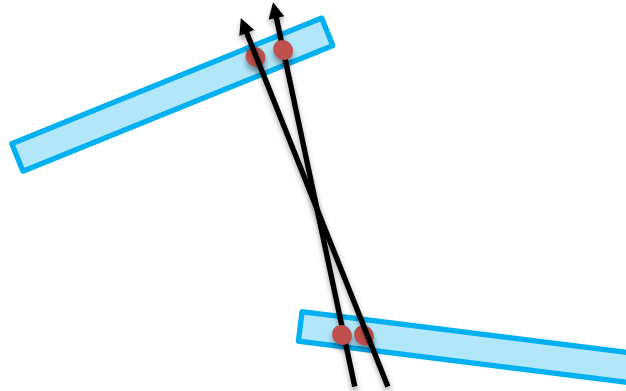


# Detection Method / Module Overlaps

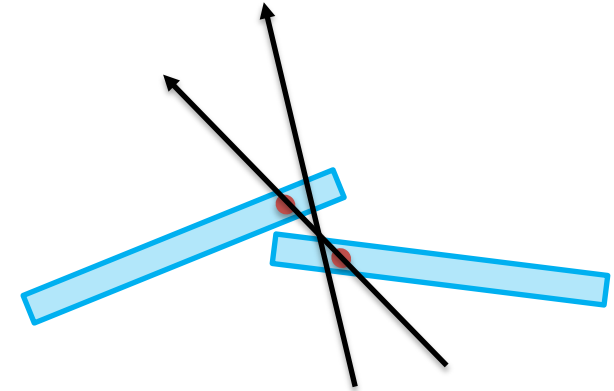
---



Ideal condition



Small variation of track saves  $\chi^2$

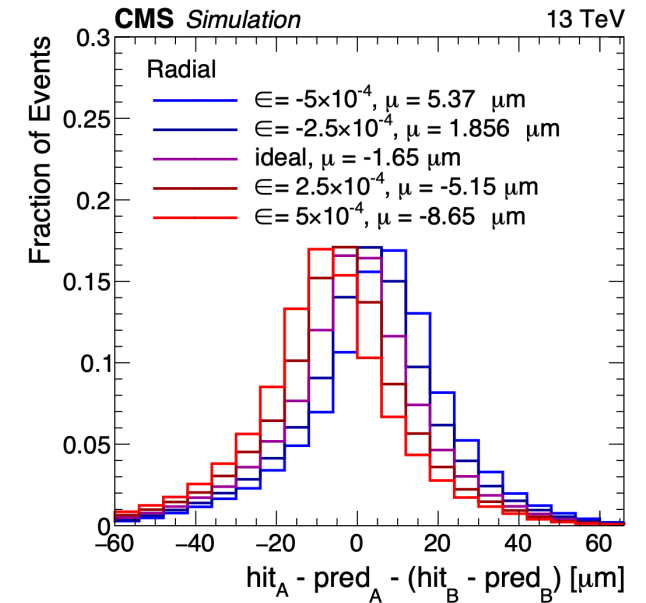
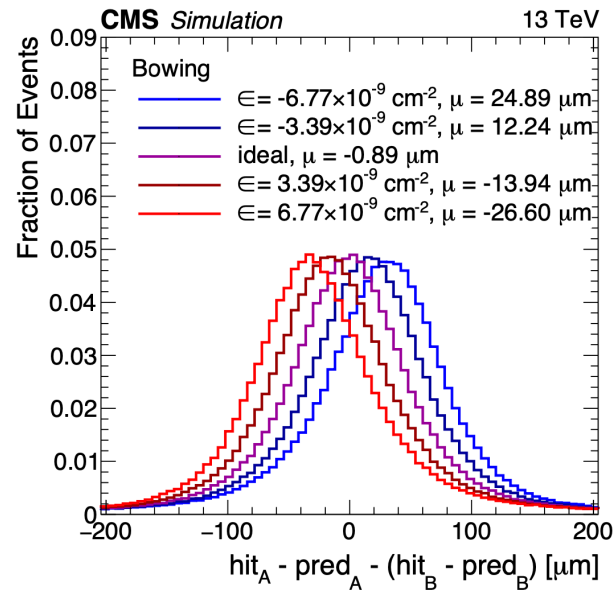
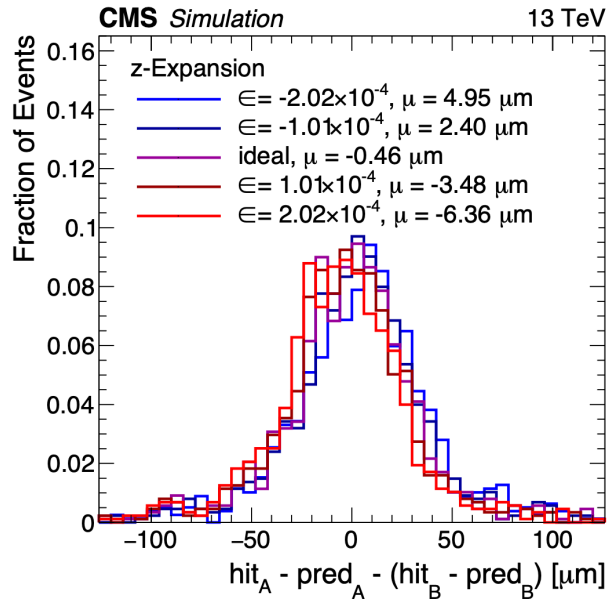


Cheating becomes expensive

Therefore,  $\Delta r_{AB}$  geometrically cancels out track extrapolation errors (due to the  $\sim$  mm distance), stripping away the flexibility of track parameters.

However, overlap tracks constitute a very small fraction of the total collision dataset. Therefore the  $\Delta r_{AB}$  is explicitly extracted as a dedicated observable to monitor radial and bowing WMs.

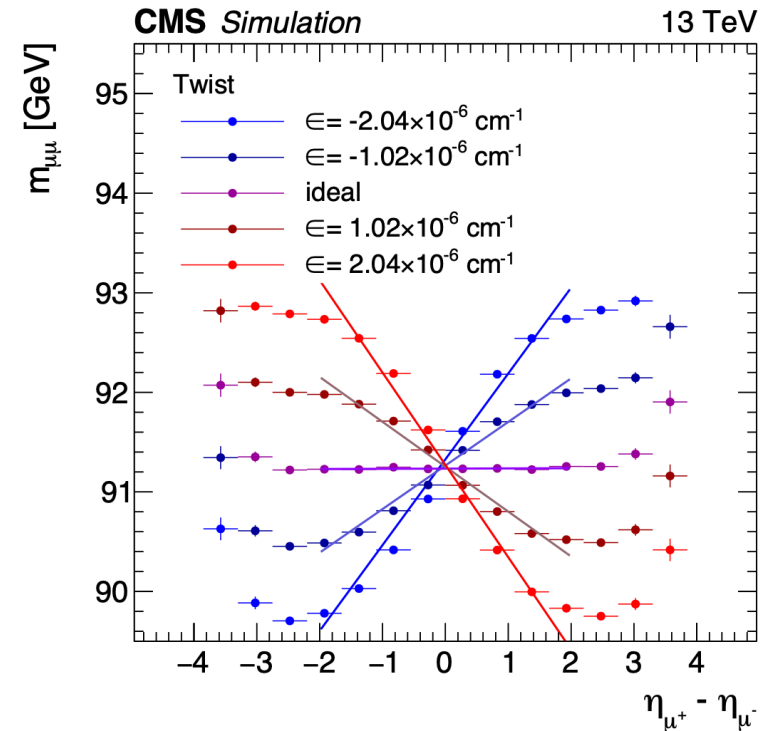
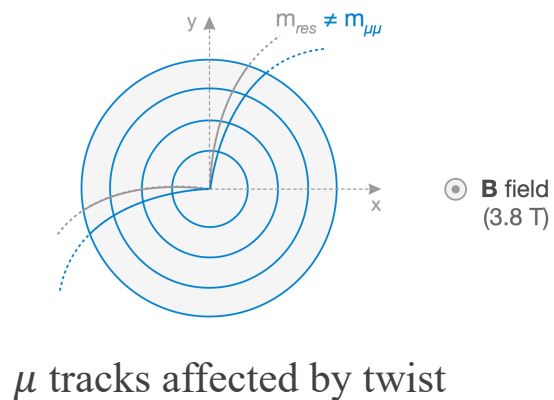
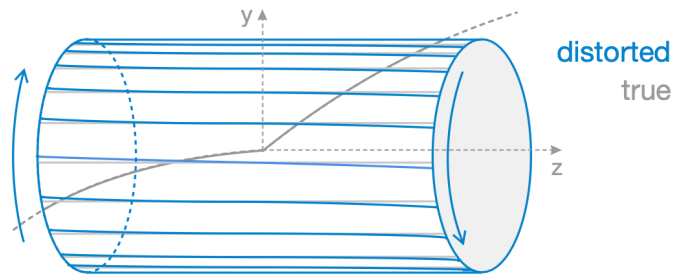
# Detection Method / Module Overlaps



z-Expansion, Bowing and Radial can be detected by Mean Shifts of  $\Delta r_{AB}$

# Detection Method / Dimuon Resonances ( $Z \rightarrow \mu\mu$ )

$Z \rightarrow$  Dimuon Resonance have a known, fixed invariant mass  $m_Z \approx 91.2$  GeV. The reconstructed mass should be independent of where the muons travel in the detector. So this measure highlights distortions that systematically bias track momenta ( $\Delta\eta_{\mu\mu}$ ).



# Alignment Method

---

In order to cancel WMs, variables listed in Detection Method are introduced into  $\chi^2$  :

Cosmic Ray:

$$\chi_{WM}^2 = \chi_{up}^2 + \chi_{low}^2 + (q_{up} - q_{low})^T V^{-1} (q_{up} - q_{low})$$

Z  $\rightarrow$   $\mu\mu$  Resonance:

$$\chi_{WM}^2 = \chi_{\mu 1}^2 + \chi_{\mu 2}^2 + [m_{\mu\mu}(q_1, q_2) - m_Z]^2 / \sigma_Z^2$$

} Add extra constraint to  $\chi^2$

Overlap Module:

$$\chi^2 = \frac{r_A^2 + r_B^2}{\sigma^2} \rightarrow \chi_{reduced}^2 = \left[ \left( r_{A0} - \frac{\partial f_A}{\partial p_A} p_A \right) - \left( r_{B0} - \frac{\partial f_B}{\partial p_B} \Delta p_B \right) \right]^2 / 2\sigma^2$$

} Original  $\chi^2$ . Improve weights of overlap region during minimization.

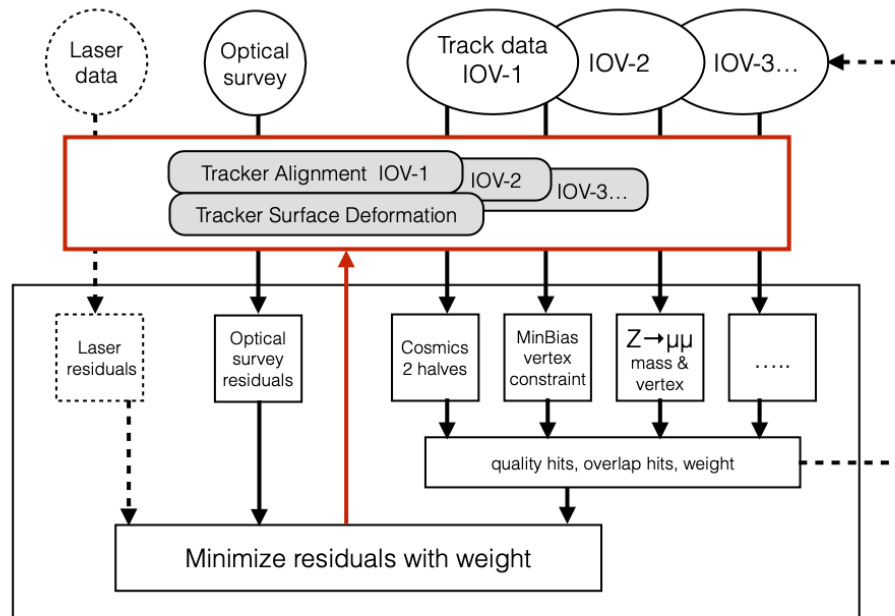
Schur Complement analytically eliminates track parameters  $q$  by solving  $\partial\chi^2/\partial q = 0$ , reducing the global matrix.

# Alignment Method

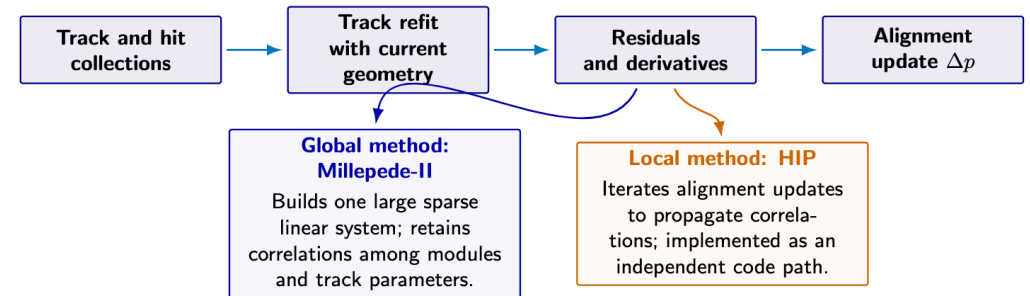
HIPPY: Local approach, explicit weighting on overlap and mass constraints

Millepede-II: Global approach, eliminates singular modes via Lagrange multipliers in sparse matrix

The modified  $\chi^2$  penalties directly eliminate singular degrees of freedom algebraically, such as uniform global scaling.



## How CMS uses alignment algorithms



Agreement between them is evidence that the result is not an artifact of one minimizer or implementation.

# Verification and Performance

---

No single plot can demonstrate that all weak modes are under control. CMS therefore validates the final geometry with several independent observables: local residual performance, track / vertex biases, dimuon mass profiles, cosmic split-track consistency and overlap residuals.

**DMR and normalized residuals**

**vertex, cosmic, overlap**

**Z →  $\mu\mu$  mass profiles**

# Verification and Performance

The grey bands at the beginning of each year indicate runs where the automated alignment updates were not active.

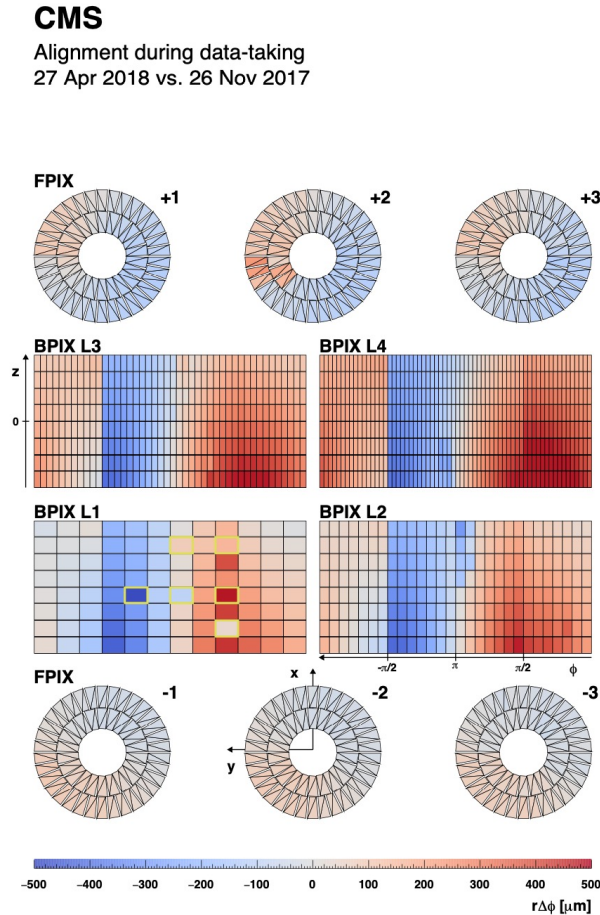
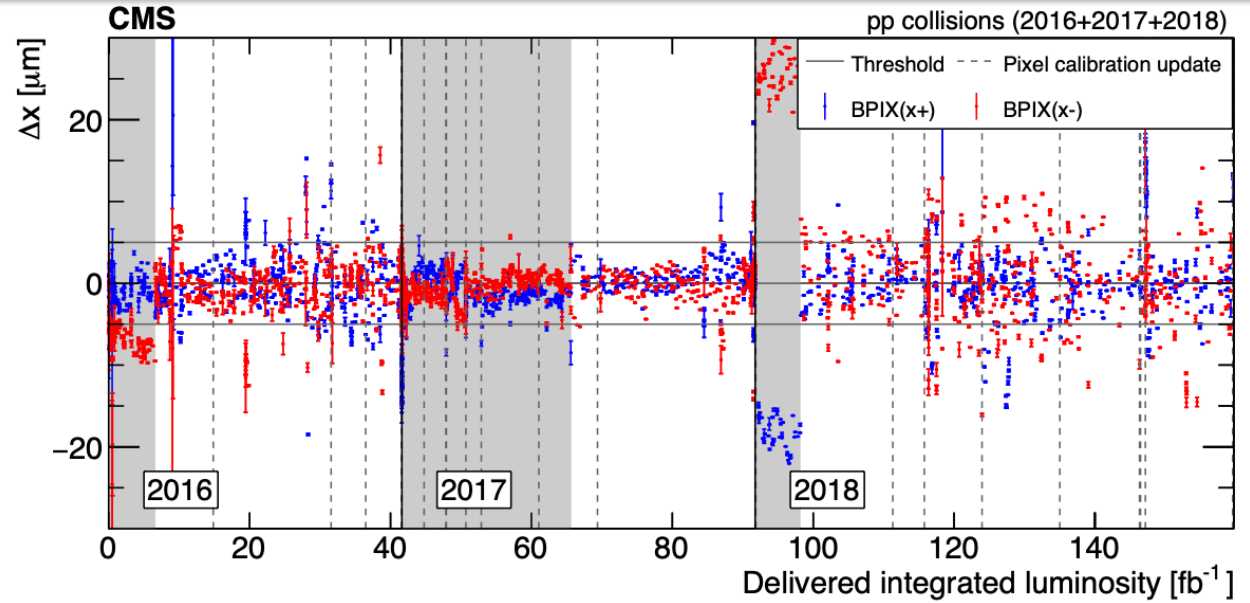


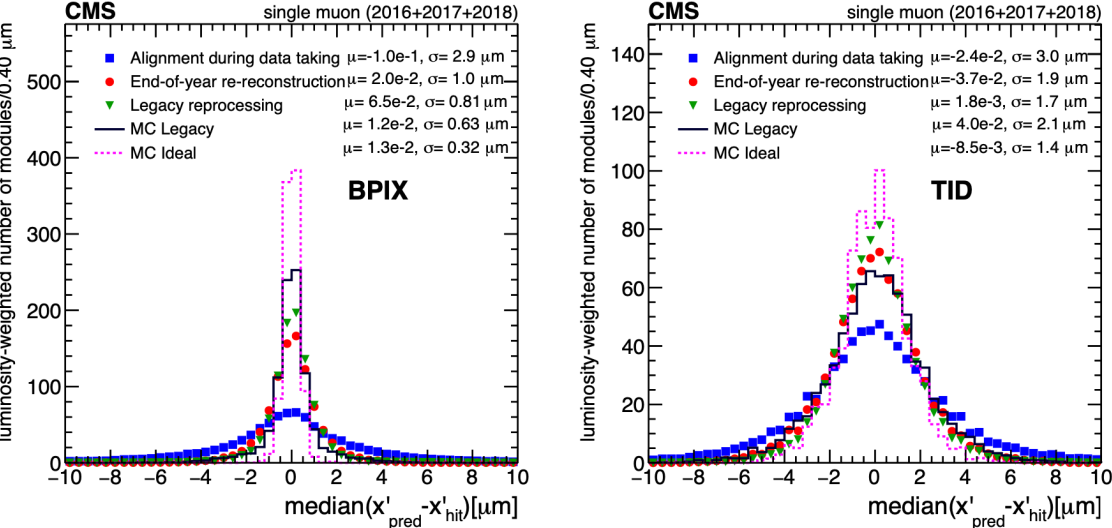
Figure 21: The value of the product  $r\Delta\phi$  for each module in the pixel detector, comparing the alignment parameters of the alignment during data taking on 26 November 2017 and on 27 April 2018. These runs correspond to the last run of 2017 and the first run of 2018 after commissioning. During this transition, several modules of layer 1 of the BPIX were replaced (indicated in yellow frames), which explains the large movements with respect to their neighbouring modules. For each of the detector components,  $r$  and  $\phi$  correspond to the global coordinate, and  $\Delta\phi$  is the shift in  $\phi$  across the two alignments resulting in the physical shift  $r\Delta\phi$  in the detector.



During data taking, CMS runs an automated low-granularity alignment in the Prompt Calibration Loop (PCL). This fit uses a small number of degrees of freedom to keep the prompt reconstruction stable against fast high-level detector movements.

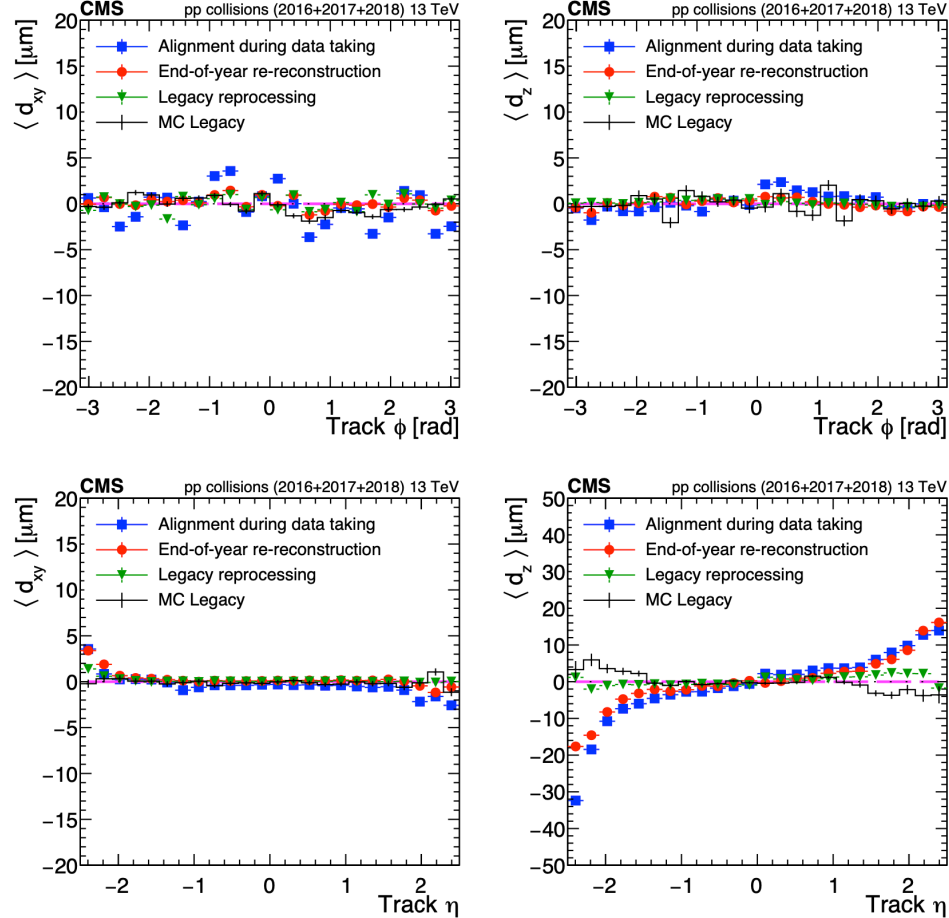
End-of-year & Legacy Reprocessing are conducted after the data-taking period with offline / high precision alignments. At this stage CMS combines much larger collision samples, cosmic tracks, dimuon resonances, and release more degrees of freedom than in prompt reconstruction.

# Verification and Performance



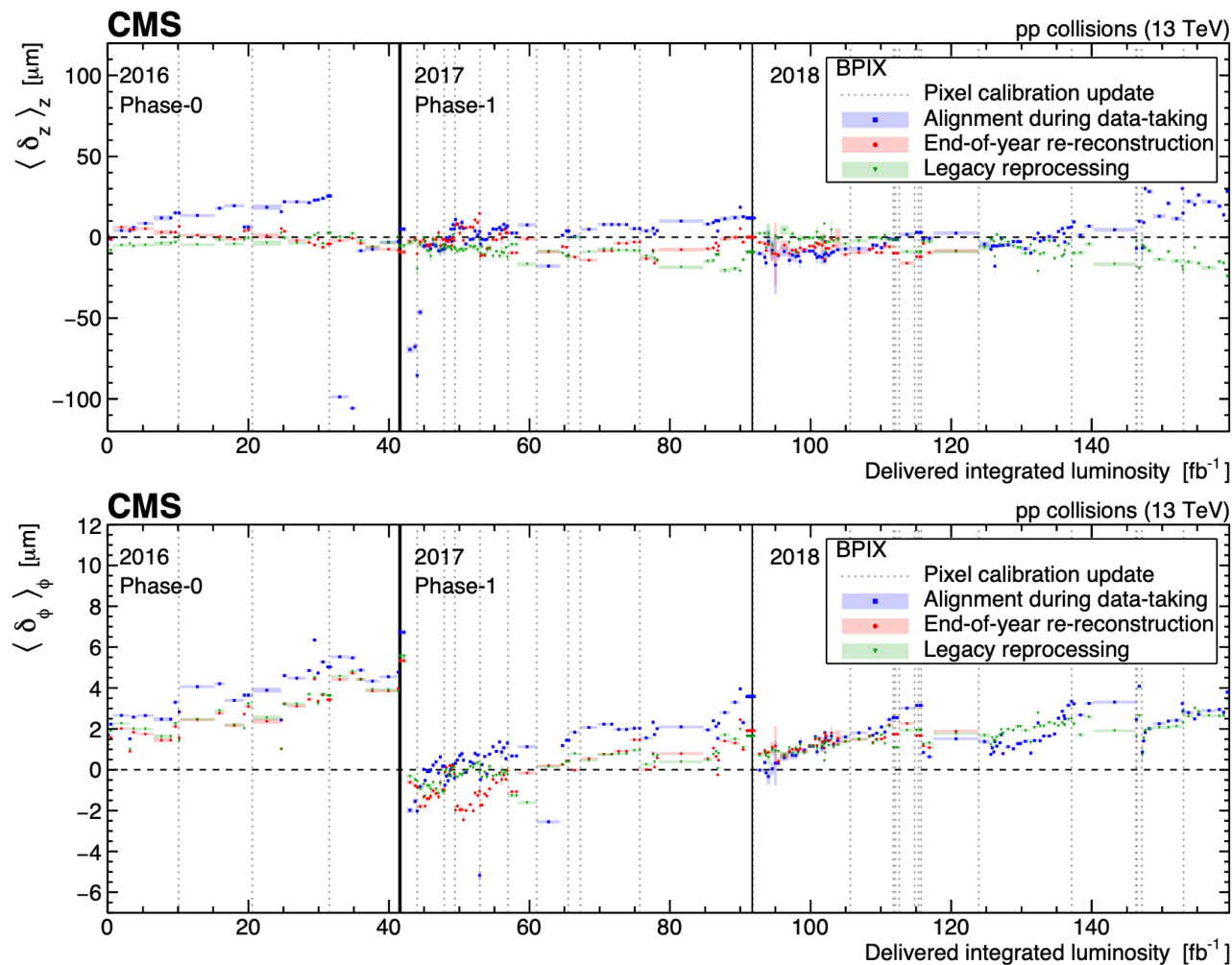
In the BPIX example, the width improves from  $2.9 \mu\text{m}$  during data taking to  $0.81 \mu\text{m}$  in legacy reprocessing. In TID it improves from  $3.0 \mu\text{m}$  to  $1.7 \mu\text{m}$ .

Also Legacy alignment strongly flattens  $d$  vs  $\phi/\eta$  distribution, especially in high- $|\eta|$  region.



They are sensitive to coherent geometry biases that can be hidden in local residual distributions

# Verification and Performance



$z$  and  $\phi$  overlap-residual monitored over delivered luminosity.

Non-zero values remain even for the legacy geometry, showing that the observable is sensitive not only to pure geometry but also to local reconstruction changes such as radiation damage to the detector.

If the remaining deviations are interpreted as pure distortions, there are approximate residual bounds of  $-105$  to  $+10$   $\mu\text{m}$  for longitudinal deform at  $z = 26$  cm, and  $-5.7$  to  $+16.5$   $\mu\text{m}$  for radial deform at  $r = 16$  cm.

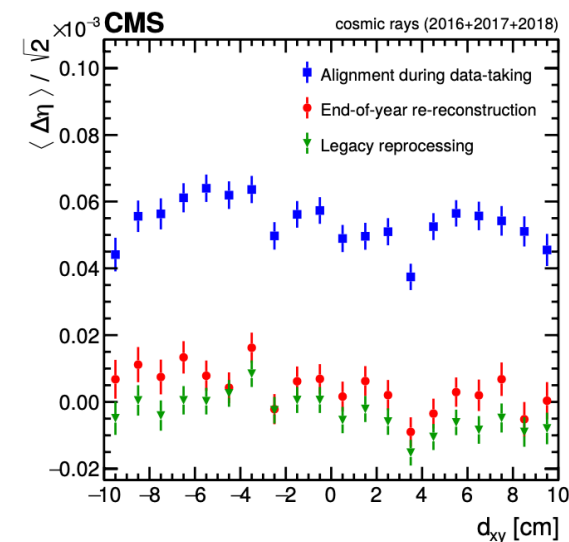
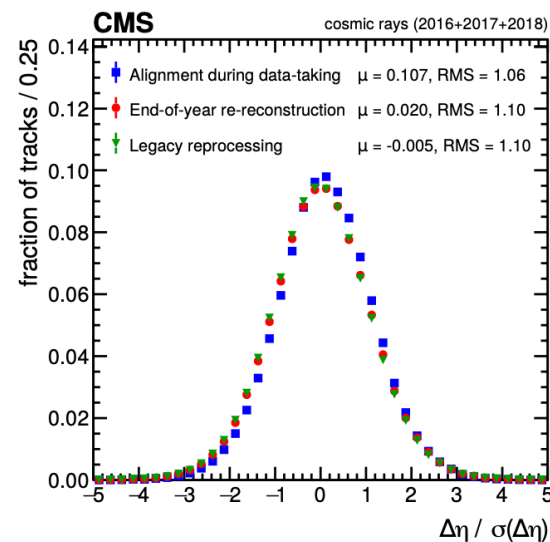
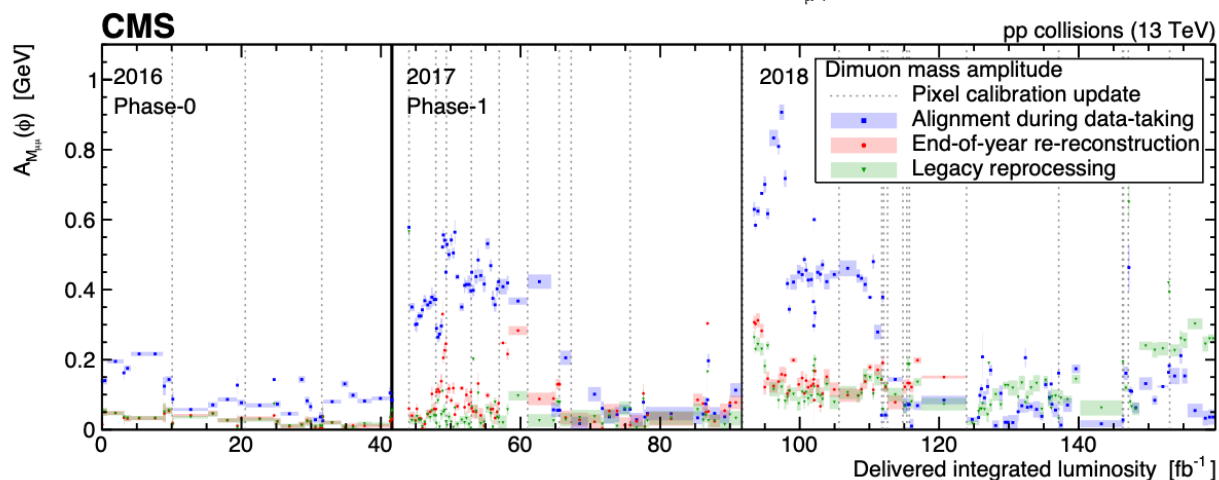
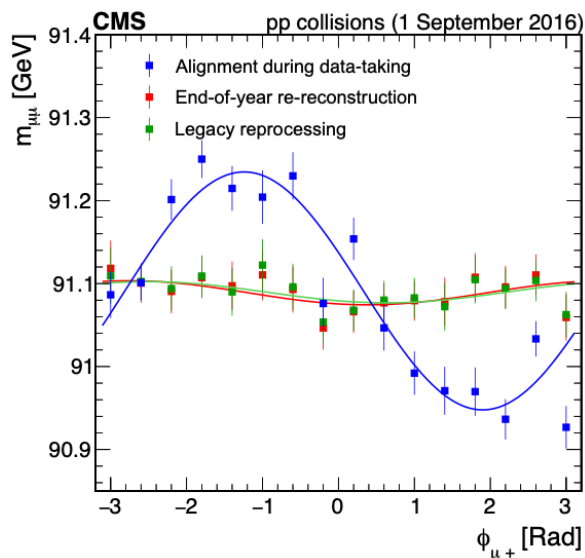
# Verification and Performance

- Dimuon Mass Amplitude (Twist Mode):

- Fitted amplitude  $A$  of  $m_{\mu\mu}(\varphi) = A_{M\mu\mu} \cos(\varphi + \varphi_0) + b$  tracks twist-like momentum bias over time.

- Cosmic Split-Track Consistency (Telescope Mode):

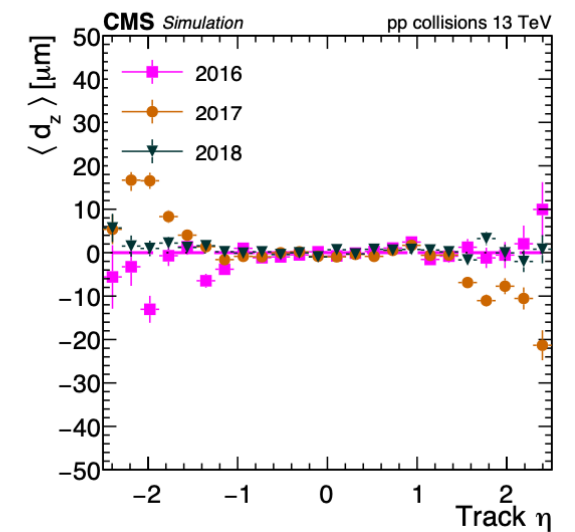
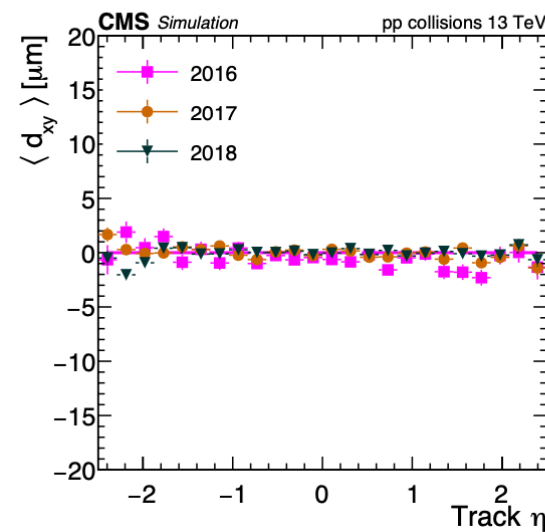
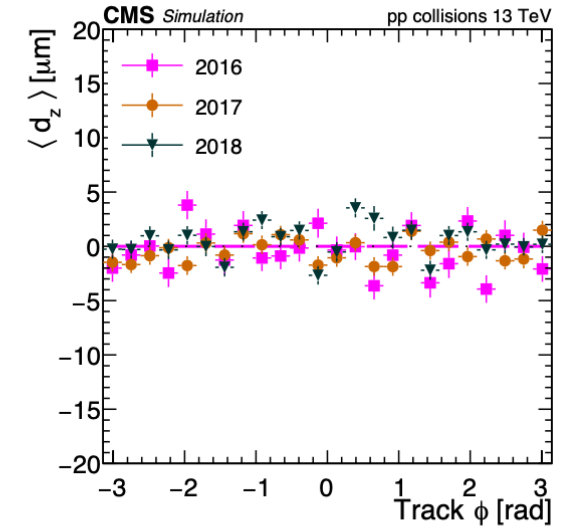
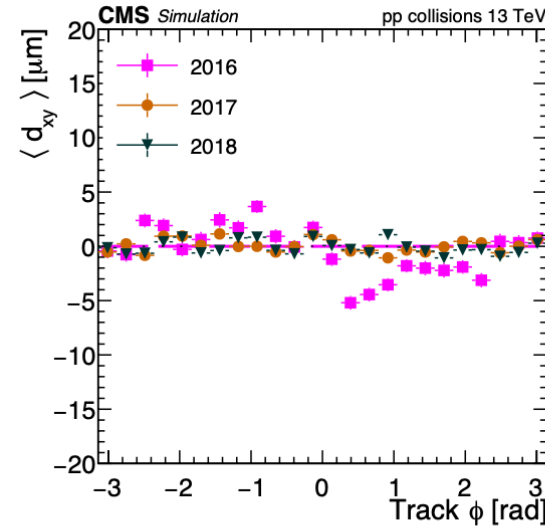
- Evaluates the difference in  $\eta$  between upper and lower halves of cosmic muons.



# Verification and Performance

For physics analyses, it is not sufficient to align only the data. The simulation must also reproduce the residual alignment performance and detector-condition effects seen in data. CMS therefore derives separate realistic alignment scenarios for 2016, 2017, and 2018 legacy MC.

The MC scenario is validated using the same families of observables as the data alignment: DMRs, cosmic split-track quantities, and track–vertex impact-parameter profiles.



# Verification and Performance

In the Run 2 legacy strategy, different years and detector partitions require different choices of high-level alignables and intervals of validity. In particular, the Phase-1 pixel detector is more sensitive to radiation-induced local reconstruction effects, so smaller pixel structures and finer IOVs are needed.

For 2018, the paper reports that a residual twist remained after the fit and was compensated with an inverted twist transformation.

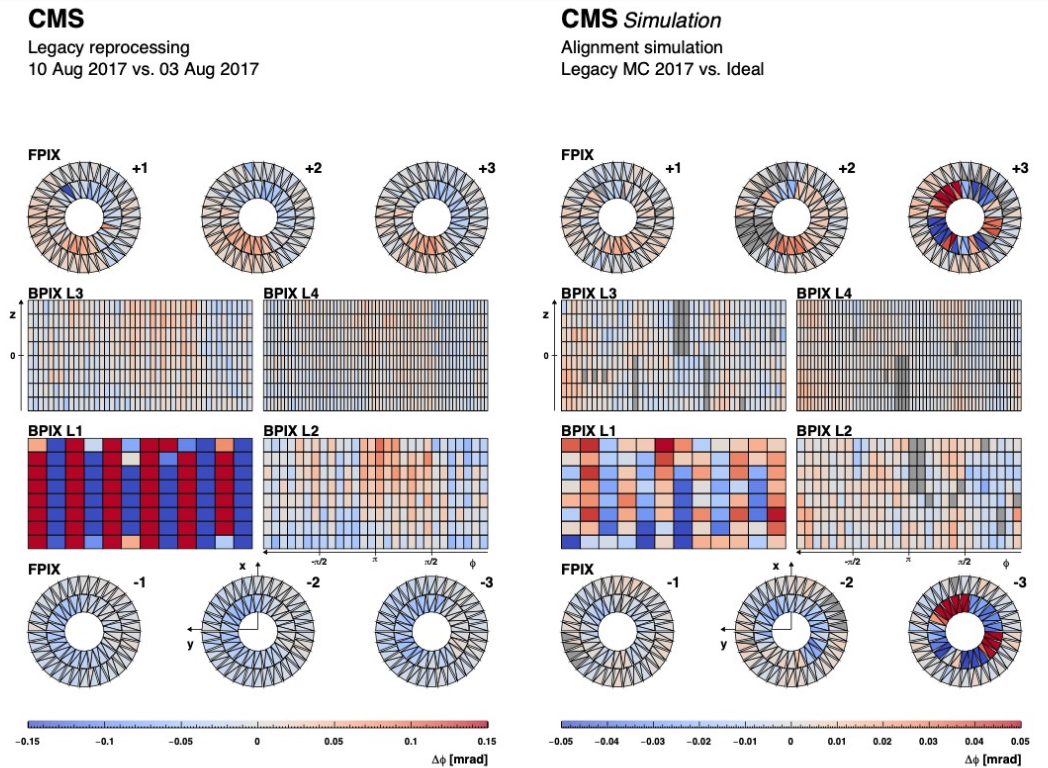


Figure 26: The value of  $\Delta\phi$  for each module in the pixel detector, comparing the alignment parameters of the legacy reprocessing on 3 and 10 August 2017 (left) and comparing the alignment based on MC simulation for 2017 and the ideal detector (right). For each of the detector components,  $\phi$  corresponds to the global coordinate. The colours denote the value of the  $\Delta\phi$  movement, as shown by the bar at the bottom. These values are capped between  $-0.15$  and  $0.15$  mrad for the alignments in data (left) and between  $-0.05$  and  $0.05$  mrad for simulation (right). In the figure on the right, modules that were inactive in the simulation are indicated in dark grey. The alternating pattern visible in layer 1 of the BPIX is caused by radiation damage that is absorbed in the modules between local calibration updates of the pixel modules. Due to the opposite orientations of the neighbouring ladders, an alternating pattern is created. Radiation damage is more severe in the first layer which is closer to the interaction point, making the pattern more visible.

# Summary

---

Standard track-based alignment is blind to Weak Modes, which systematically bias physics observables while preserving the track  $\chi^2$ .

CMS eliminates undefined degrees of freedom mathematically via Lagrange multipliers in global fits and dynamic pseudo-measurements in local updates. Misalignments are under strict control in both running and reprocessing.

Thanks

# References

---

- [1] CMS Collaboration, “Strategies and performance of the CMS silicon tracker alignment during LHC Run 2,” Nucl. Instrum. Meth. A 1037 (2022) 166795, arXiv:2111.08757.
- [2] CMS Collaboration, “Alignment of the CMS tracker with LHC and cosmic ray data,” JINST 9 (2014) P06009, arXiv:1403.2286.
- [3] V. Blobel, “Software alignment for tracking detectors,” Nucl. Instrum. Meth. A 566 (2006) 5–13.
- [4] CMS Collaboration, “CMS Run 3 tracker-alignment proceeding”, arXiv:2401.01261.



# Alignment inputs: why several track topologies are required

Different samples break different degeneracies

---

Input	Primary weak-mode use
$Z/Y \rightarrow \mu\mu$	mass and vertex constraints; twist-like momentum bias
Cosmic muons	top/bottom split-track consistency; telescope, sagitta, skew
Overlap hits	radial/z scale and bowing through double residuals
Inclusive tracks	high-statistics local alignment and monitoring
Isolated muons	precise tracking-performance validation

# Observable assignment for the nine modes

This table should be read together with the geometry schematic

Geometric family	Representative modes	Sensitive observable	Measured quantity
Scale in z or r	z expansion, radial	overlap residuals in z or $\varphi$	mean of residual double difference
$\varphi$ displacement vs z	twist	$Z \rightarrow \mu\mu$ mass profile vs $\Delta\eta$ or $\varphi$	slope or cosine amplitude of reconstructed mass
z displacement vs r	telescope	cosmic split tracks	mean $\Delta\theta/\sigma(\Delta\theta)$ or impact-parameter trend
r displacement vs z	bowing	overlap residuals	mean shift in overlap residual distribution
$\varphi$ displacement vs r	layer rotation	cosmic split tracks	mean $\Delta(q/pT)$
$\varphi$ -dependent coherent terms	skew, elliptical, sagitta	cosmic split tracks vs $\varphi$	fit amplitude in $\Delta dz$ , $\Delta dxy$ , or $\Delta\varphi$ profiles

# $\phi$ -dependent modes in detail

Skew, elliptical distortion, and sagitta are quantified by fitted profiles

---

Mode	Geometry	Cosmic-splitting observable	Fit form / metric
Skew	$\Delta z = \varepsilon \cos(\varphi + \varphi_0)$	$\Delta dz / \sqrt{2}$ versus $\varphi$	$A \tanh[B(\varphi + C)]$
Elliptical	$\Delta r = \varepsilon r \cos(2\varphi + 2\varphi_0)$	$\Delta dxy / \sqrt{2}$ versus $\varphi$	$-A \sin(2\varphi + B)$
Sagitta	$\Delta \varphi = \varepsilon \cos(\varphi + \varphi_0)$	$\Delta \varphi / \sqrt{2}$ versus $\varphi$	$-A \cos(\varphi + B)$

# MillePede-II and HipPy: comparison

Feature	MillePede-II	HipPy
Fit strategy	Global linearized least-squares system; track-parameter correlations are retained when solving for $\Delta p$	Local hit-and-impact-point updates; correlations are approximated by repeated iterations
Numerics	Large sparse normal equations; exact or iterative solvers depending on parameter count	Many small local matrix inversions; no single large global inversion
Track model	Uses General Broken Lines for trajectory refit and multiple scattering	Uses CMS track-refitting infrastructure directly
Practical role	Main tool for large Run 2 global fits and legacy reprocessing	Independent implementation; useful for cross-checks and flexible constraints
Cross-check meaning	Tests a globally correlated solution	Tests whether a different approximation and code path converges to compatible geometry

# Future Upgrade

---

The Run 3 proceeding reports that the same track-based alignment logic continues, with MillePede-II and HipPy used as complementary tools. The most relevant operational change is the deployment of a higher-granularity Pixel Prompt Calibration Loop alignment in September 2022.

The prompt alignment granularity increased from 36 Pixel high-level-structure parameters to approximately 5000 Pixel ladder/panel parameters. This will bring more detector-condition and weak-mode control into the prompt reconstruction workflow.